

Phosphido-Bridged Heterobimetallic Complexes Derived from Niobocene and Diiron Nonacarbonyl. Crystal Structure of $\text{Cp}_2\text{Nb}(\mu\text{-PPh}_2)(\mu\text{-CO})\text{Fe}(\text{CO})_3$

Pascal Oudet, Marek M. Kubicki,* and Claude Moïse

Laboratoire de Synthèse et d'Electrosynthèse Organométalliques (Unité de recherche associée au CNRS 1685), Faculté des Sciences, Université de Bourgogne, 6 Boulevard Gabriel, 21000 Dijon, France

Received March 17, 1994[®]

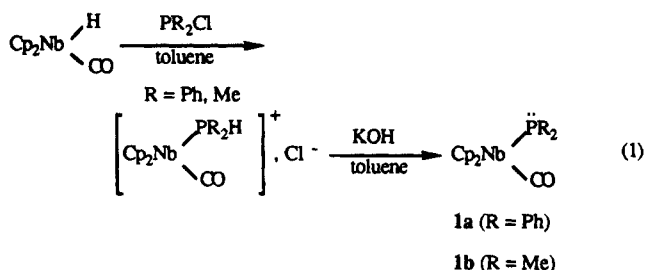
The terminal phosphido complexes $\text{Cp}_2\text{Nb}(\text{CO})\text{PR}_2$ ($\text{R} = \text{Ph}, \text{Me}$) prepared by published procedures react with $\text{Fe}_2(\text{CO})_9$ to give a mixture of mono- and dibridged compounds $\text{Cp}_2\text{Nb}(\text{CO})(\mu\text{-PR}_2)\text{Fe}(\text{CO})_4$ and $\text{Cp}_2\text{Nb}(\mu\text{-PR}_2)(\mu\text{-CO})\text{Fe}(\text{CO})_3$. Removal by photolysis of one CO from the monobridged complexes produced the dibridged compounds. All new mono- and dimetallic complexes have been characterized by ^1H and ^{31}P NMR and IR spectroscopy, and EHMO calculations have been carried out on dimethylphosphido derivatives. The complex $\text{Cp}_2\text{Nb}(\mu\text{-PPh}_2)(\mu\text{-CO})\text{Fe}(\text{CO})_3$ crystallizes in the triclinic space group $P\bar{1}$ with $a = 7.936(7)$ Å, $b = 10.010(7)$ Å, $c = 15.153(8)$ Å, $\alpha = 91.26(5)^\circ$, $\beta = 92.80(6)^\circ$, $\gamma = 101.23(6)^\circ$, $V = 1178.8$ Å³, $R = 0.046$, and $Z = 2$. The molecular structure reveals a short distance between metallic centers ($\text{Nb-Fe} = 2.884(2)$ Å), indicating the existence of a metal-metal bond. Dibridged complexes $\text{Cp}_2\text{Nb}(\mu\text{-PR}_2)(\mu\text{-CO})\text{Fe}(\text{CO})_3$ ($\text{R} = \text{Ph}, \text{Me}$) did not react with CO, but a good donor ligand (PMe_2Ph) displaced the metal-metal bond, leading to new phosphido-monobridged compounds without a metal-metal bond, $\text{Cp}_2\text{Nb}(\text{CO})(\mu\text{-PR}_2)\text{Fe}(\text{CO})_3(\text{PMe}_2\text{Ph})$.

Introduction

Terminal phosphido transition-metal complexes have been shown to be good precursors for the preparation of bimetallic compounds.¹⁻⁵ Some terminal diphosphido complexes derived from bent metallocenes are known in the chemistry of group 4 metals (Zr^{IV} , Hf^{IV} , metal d^0).^{5,6} More recently monophosphido complexes of group 6 metallocenes (Mo^{IV} , W^{IV} , metal d^2)^{7,8} of the type $\text{Cp}_2\text{M}(\text{H})(\text{PPh}_2)$ have been prepared. It has been shown that they easily form the monobridged ($\mu\text{-PPh}_2$) structures without a metal-metal bond and dibridged ($\mu\text{-PPh}_2$, $\mu\text{-H}$) structures.⁹ We have already reported on an easy synthesis of equivalent complexes in the chemistry of group 5 metallocenes (Nb^{III} , metal d^2): $\text{Cp}_2\text{Nb}(\text{CO})\text{PPh}_2$ (**1a**) from $\text{Cp}_2\text{Nb}(\text{H})(\text{CO})$ and PPh_2Cl .¹⁰

Chemical, structural, and theoretical studies of these d^2 terminal phosphido compounds showed the existence

of the "transition metal gauche effect"^{9,11,12} leading to an enhanced nucleophilicity¹² of the phosphorus atom. The new dimethylphosphido niobocene complex **1b** is obtained by following eq 1.



We report here on the properties of dinuclear mono- and dibridged systems formed in reactions of the complexes $\text{Cp}_2\text{Nb}(\text{CO})\text{PR}_2$ ($\text{R} = \text{Ph}, \text{Me}$) with $\text{Fe}_2(\text{CO})_9$.

Experimental Section

General Procedures. All reactions were carried out under an argon atmosphere with use of standard Schlenk techniques. The solvents and eluents were distilled under argon from sodium and benzophenone immediately before use. Column chromatography was performed under argon and with silica gel (70-230 mesh). Elemental (C, H) analyses were performed by the "Service Central d'Analyse du CNRS" (Gif sur Yvette, France).

Infrared spectra were recorded with a Perkin-Elmer 589 B spectrophotometer. ^1H and ^{31}P NMR spectra were recorded on Bruker WM 400 spectrometers; chemical shifts are given in ppm relative to Me_4Si (^1H) or (external) H_3PO_4 (^{31}P). $\text{Cp}_2\text{-}$

(11) Bonnet, G.; Kubicki, M. M.; Moïse, C.; Lazzaroni, R.; Salvadori, P.; Vitulli, G. *Organometallics* **1992**, *11*, 964.

(12) Buhro, W. E.; Zwick, B. D.; Georgiou, S.; Hutchinson, J. P.; Gladysz, J. A. *J. Am. Chem. Soc.* **1988**, *110*, 2427 and references therein.

[®] Abstract published in *Advance ACS Abstracts*, September 15, 1994.

(1) Carty, A. J.; MacLaughlin, S. A.; Nucciarone, D. In *Methods in Stereochemical Analysis*; Marchand, A. P., Ed.; Phosphorus-31 NMR Spectroscopy in Stereochemical Analysis 8; VCH: Deerfield Beach, FL, 1987; Chapter 16.

(2) Stephan, D. W. *Coord. Chem. Rev.* **1989**, *95*, 41.

(3) Baker, R. T.; Fultz, W. C.; Marder, T. B.; Williams, I. D. *Organometallics* **1990**, *9*, 2357.

(4) Casey, C. P.; Bullock, R. M. *Organometallics* **1984**, *3*, 1102.

(5) Baker, R. T.; Tulip, T. H.; Wreford, S. S. *Inorg. Chem.* **1985**, *24*, 1379.

(6) (a) Wade, S. R.; Wallbridge, M. G. H.; Wiley, J. R. *J. Chem. Soc., Dalton Trans.* **1983**, 2555. (b) Baker, R. T.; Whitney, J. F.; Wreford, S. S. *Organometallics* **1983**, *2*, 1049. (c) Targos, T. S.; Rosen, R. P.; Whittle, R. R.; Geoffroy, G. L. *Inorg. Chem.* **1985**, *24*, 1375. (d) Vaughan, G. A.; Hillhouse, G. L.; Rheingold, A. L. *Organometallics* **1989**, *8*, 1760.

(7) Barré, C.; Kubicki, M. M.; Leblanc, J. C.; Moïse, C. *Inorg. Chem.* **1990**, *29*, 5244.

(8) Kubicki, M. M.; Kergoat, R.; Cariou, M.; Guerschais, J. E.; L'Haridon, P. *J. Organomet. Chem.* **1987**, *322*, 357.

(9) Barré, C.; Boudot, P.; Kubicki, M. M.; Moïse, C. Submitted for publication in *Inorg. Chem.*

(10) Bonnet, G.; Lavastre, O.; Leblanc, J. C.; Moïse, C. *New J. Chem.* **1988**, *12*, 551.

Table 1. Crystallographic Data for $\text{Cp}_2\text{Nb}(\mu\text{-PPh}_2)(\mu\text{-CO})\text{Fe}(\text{CO})_3$ (3a**)**

mol formula	$\text{C}_{26}\text{H}_{20}\text{O}_4\text{PNbFe}$
fw	576.17
cryst syst	triclinic
space group	$P\bar{1}$ (No. 2)
cell dimens	
<i>a</i> , Å	7.936(7)
<i>b</i> , Å	10.010(7)
<i>c</i> , Å	15.153(8)
β , deg	92.80(6)
<i>V</i> , Å ³	1178.8
<i>Z</i>	2
ρ_{calcd} , g cm ⁻³	1.623
<i>F</i> (000)	580
radiation, Å	$\lambda(\text{Mo K}\alpha) = 0.71073$
scan type	$\omega-2\theta$
scan speed, deg min ⁻¹	1.8–16.5
scan width, deg	$\Delta\omega = 1.2 + 0.34 \tan \theta$
reflections measd	<i>h</i> , -9 to +9; <i>k</i> , -11 to +11; <i>l</i> , 0–18
θ range, deg	2–25
linear abs, μ , cm ⁻¹	11.764
no. of rflns measd	4336
decay, %	-1.3
abs cor (DIFABS), abs _{min} –abs _{max}	0.7423–1.4559
cutoff for obsd data	$I \geq 3\sigma(I)$
no. of unique obsd data (NO)	3296
no. of variables (NV)	299
<i>R</i> (<i>F</i>)	0.046
<i>R</i> _w (<i>F</i>)	0.056
<i>p</i> in $1/\sigma(F_o)^2 = [\sigma(I)^2 + (pF_o^2)^2]^{-1/2}$	0.7
GOF	1.919
ρ_{max} , e/Å ³	0.96 (near Nb atom)

$\text{Nb}(\text{CO})\text{H}$ was prepared according to the literature procedure.¹³ $\text{Fe}_2(\text{CO})_9$ (Aldrich) and PMe_2Cl (Strem) have been used as received.

Preparation of $[\text{Cp}_2\text{Nb}(\text{CO})\text{PMe}_2\text{H}]^+\text{Cl}^-$. To a toluene solution (20 mL) of $\text{Cp}_2\text{Nb}(\text{CO})\text{H}$ (0.5 g, 2 mmol) was added PMe_2Cl (0.2 g, 2 mmol). An orange precipitate was instantaneously formed. After 30 min of stirring it was filtered, washed with pentane, and dried under vacuum (yield 0.56 g, 80%). NMR (δ , ppm): ¹H (CD_3COCD_3) 5.71 (d, *J* = 2.6 Hz, Cp), 5.20 (dh, *J* = 6.4, 354 Hz, PH), 1.68 (dd, *J* = 6.4, 10, CH₃); ³¹P (CD_3COCD_3) -15. IR ($\nu(\text{CO})$, CH_2Cl_2): 1960 cm⁻¹. This complex is extremely air sensitive.

Preparation of **1b.** A saturated aqueous solution of KOH (10 mL) was added to the dried salt $[\text{Cp}_2\text{Nb}(\text{CO})\text{PMe}_2\text{H}]^+\text{Cl}^-$ (0.5 g, 1.43 mmol) prepared from $\text{Cp}_2\text{Nb}(\text{CO})\text{H}$ and PMe_2Cl . The mixture was stirred for 30 min. The product was extracted with 2 × 15 mL of toluene, and the organic layer was separated and evaporated, giving 0.27 g of a green powder (yield 60%). The complex **1b** is extremely air sensitive.

Preparation of **2a and **3a**.** To a toluene solution (30 mL) of $\text{Cp}_2\text{Nb}(\text{CO})\text{PPh}_2$ (**1a**; 0.5 g, 1.14 mmol) was added $\text{Fe}_2(\text{CO})_9$ (0.4 g, 1.14 mmol). The mixture was stirred for 2 h at room temperature. The solvent was removed under vacuum, and the crude product was washed with 3 × 15 mL of pentane to remove $\text{Fe}(\text{CO})_5$. The reaction products were dissolved in 8 mL of toluene and chromatographed. Elution with toluene led to **2a**. Recrystallization from CH_3COCH_3 gave deep orange crystals of **2a** in 40% yield (0.28 g). The complex **3a** was eluted with THF. Recrystallization from CH_3COCH_3 gave deep red crystals of **3a** in 30% yield (0.20 g). The complex $\text{Cp}_2\text{Nb}(\mu\text{-CO})(\mu\text{-PPh}_2)\text{Fe}(\text{CO})_3$ (**3a**) can be prepared by UV irradiation with a Hanau TQ 150 lamp of a THF solution (60 mL) of $\text{Cp}_2\text{Nb}(\text{CO})(\mu\text{-PPh}_2)\text{Fe}(\text{CO})_4$ (**2a**; 0.3 g, 0.49 mmol). Freeze-thaw cycles removed the CO generated by the photoreaction during irradiation. The reaction was monitored by IR spectroscopy. The complex **3a** was obtained quantitatively (0.28 g) after 15 min of irradiation. The complex **2a** is air sensitive. Anal. Calcd for $\text{C}_{27}\text{H}_{20}\text{O}_5\text{PNbFe}$ (**2a**): C, 53.67; H, 3.33. Found: C,

Table 2. Positional Parameters and Their Estimated Standard Deviations for $\text{Cp}_2\text{Nb}(\mu\text{-PPh}_2)(\mu\text{-CO})\text{Fe}(\text{CO})_3$ (3a**)^a**

atom	<i>x</i>	<i>y</i>	<i>z</i>	<i>B</i> _{eq} (Å ²)
Nb	0.23434(7)	0.52259(6)	0.28063(4)	1.95(1)
Fe	-0.0126(1)	0.6934(1)	0.24392(7)	2.65(2)
P	0.2639(2)	0.7560(2)	0.2214(1)	2.09(3)
CP1	0.3364	0.5413	0.4100	
CP2	0.2447	0.3829	0.1780	
O1	-0.1604(7)	0.4257(6)	0.3190(4)	4.9(1)
O2	-0.1510(8)	0.7562(7)	0.4119(4)	5.7(2)
O3	-0.0402(8)	0.9650(6)	0.1894(5)	5.9(2)
O4	-0.2126(8)	0.5488(7)	0.0911(4)	5.9(2)
C1	-0.0404(9)	0.5017(7)	0.2950(5)	3.1(1)
C2	-0.0947(9)	0.7296(8)	0.3456(5)	3.7(2)
C3	-0.027(1)	0.8566(8)	0.2102(6)	3.8(2)
C4	-0.1334(9)	0.6066(7)	0.1511(6)	3.7(2)
C11	0.327(1)	0.4216(7)	0.4103(4)	3.4(2)
C12	0.200(1)	0.4904(8)	0.4337(5)	3.7(2)
C13	0.261(1)	0.6279(7)	0.4246(5)	3.2(1)
C14	0.4258(9)	0.6481(7)	0.3953(4)	3.2(1)
C15	0.4695(9)	0.5185(8)	0.3861(5)	3.5(2)
C16	0.368(1)	0.4548(8)	0.1541(5)	4.2(2)
C17	0.365(1)	0.3532(8)	0.2154(6)	4.7(2)
C18	0.197(1)	0.2938(8)	0.2251(6)	5.2(2)
C19	0.095(1)	0.3567(9)	0.1683(6)	5.5(2)
C20	0.199(1)	0.4561(8)	0.1271(5)	4.1(2)
C21	0.3812(8)	0.9083(6)	0.2842(4)	2.2(1)
C22	0.309(1)	0.9586(7)	0.3561(5)	3.1(1)
C23	0.398(1)	1.0675(7)	0.4072(5)	3.8(2)
C24	0.562(1)	1.1305(8)	0.3864(5)	4.3(2)
C25	0.635(1)	1.0809(8)	0.3154(6)	4.3(2)
C26	0.548(1)	0.9714(7)	0.2645(5)	3.4(2)
C27	0.3352(9)	0.7875(6)	0.1099(4)	2.6(1)
C28	0.501(1)	0.7720(7)	0.0885(5)	3.3(2)
C29	0.559(1)	0.7956(8)	0.0047(5)	4.3(2)
C30	0.454(1)	0.8365(8)	-0.0597(5)	4.8(2)
C31	0.289(1)	0.8513(8)	-0.0400(5)	4.4(2)
C32	0.230(1)	0.8265(7)	0.0446(5)	3.5(2)

^a Anisotropically refined atoms are given in the form of the isotropic equivalent displacement parameter, defined as $\frac{1}{3}[a^2B(1,1) + b^2B(2,2) + c^2B(3,3) + ab(\cos \gamma)B(1,2) + ac(\cos \beta)B(1,3) + bc(\cos \alpha)B(2,3)]$. CP(1) and CP(2) represent the gravity centers of the C11–C15 and C16–C20 cyclopentadienyl rings.

54.07; H, 3.31. Anal. Calcd for $\text{C}_{26}\text{H}_{20}\text{O}_4\text{PNbFe}$ (**3a**): C, 54.20; H, 3.49. Found: C, 53.75; H, 3.60.

Preparation of **2b and **3b**.** They were prepared by a procedure similar to that for **2a** and **3a** in 60% and 10% yields, respectively. The synthesis of **3b** by UV irradiation of **2b** is quantitative after 1 h. The complex **2b** is air sensitive. Anal. Calcd for $\text{C}_{17}\text{H}_{16}\text{O}_5\text{PNbFe}$ (**2b**): C, 42.53; H, 3.36. Found: C, 42.39; H, 3.33. Anal. Calcd for $\text{C}_{16}\text{H}_{16}\text{O}_4\text{PNbFe}$ (**3b**): C, 42.51; H, 3.57. Found: C, 41.95; H, 3.80.

Preparation of **4a.** To a toluene solution (20 mL) of $\text{Cp}_2\text{Nb}(\mu\text{-CO})(\mu\text{-PPh}_2)\text{Fe}(\text{CO})_3$ (**3a**; 0.1 g, 0.17 mmol) was added a small excess of PMe_2Ph . The mixture was refluxed for 3 h. The solvent was removed under vacuum, and the solid residue was washed with pentane (2 × 10 mL). Recrystallization from toluene gave a clear maroon powder of **4a** in 50% yield (0.06 g). The complex **4a** is extremely air sensitive.

Preparation of **4b.** The procedure was similar to that for **4a** to give **4b** in 50% yield. The complex **4b** is extremely air sensitive.

X-ray Structure Determination. X-ray-quality crystals of **3a** were grown from acetone solution. A red irregularly shaped crystal (approximate dimensions 0.40 × 0.15 × 0.10 mm) was mounted on an Enraf-Nonius CAD4 diffractometer. The pertinent crystallographic data are summarized in Table 1. The unit cell was determined and refined from 25 randomly selected reflections obtained by use of the CAD4 automatic routines. Intensities were corrected for Lorentz and polarization effects. All calculations were carried out by use of the Enraf-Nonius SDP package with neutral-atom scattering factors. The structure was solved and refined by conventional three-dimensional Patterson, difference Fourier, and full-

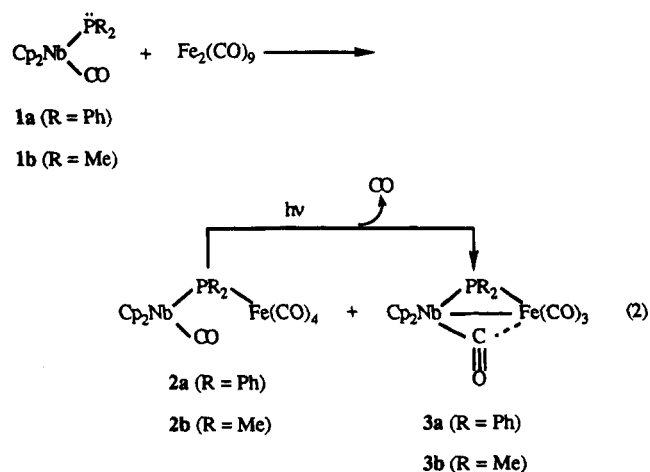
(13) Foust, D. F.; Rogers, R. D.; Rausch, M. D.; Atwood, J. L. *J. Am. Chem. Soc.* **1982**, *104*, 5646.

matrix least-squares methods. An empirical absorption correction (DIFABS) was applied after isotropic refinement of all atoms. All non-hydrogen atoms were further refined with anisotropic thermal parameters. The positions of hydrogen atoms were calculated by the HYDRO program of SDP. These atoms were included in the final calculations in a riding model with $B_{1\text{iso}}$ fixed at $1.3B_{\text{eq}}$ for the carbon atoms bearing them. The coordinates of non-hydrogen atoms are given in Table 2.

EHMO Calculations. Extended Hückel molecular orbital calculations¹⁴ were performed on the complexes **1b**, **2b**, **3b**, and **4b** (with a PH_3 model instead of PMe_2Ph). The stable conformational geometry of **1b** was derived from the crystallographic structure of $\text{Cp}_2\text{Nb}(\text{CO})\text{P}^i\text{PrPh}$.¹¹ Those of **2b** and **4b** were based on the structures of $\text{Cp}_2\text{Nb}(\text{CO})(\mu\text{-PMe}_2)\text{W}(\text{CO})_4(\text{PMe}_2\text{Ph})$ ¹⁵ and $\text{Cp}_2\text{Nb}(\text{CO})(\mu\text{-PPh}_2)\text{Cr}(\text{CO})_5$ ¹⁶ as well as on the typical geometry of an $\text{Fe}(\text{CO})_4$ fragment. The parameters found in the structure of **3a** reported here were used for the calculations of **3b**. The atomic functions were those contained in the data file of the CACAO package.¹⁷

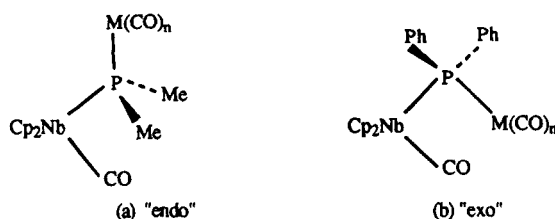
Results and Discussion

Synthesis. The niobophosphines **1** react rapidly at room temperature with $\text{Fe}_2(\text{CO})_9$ in toluene solution, leading to a mixture of the mono- and dibridged phosphido complexes **2** and **3**, respectively (eq 2).



The relative abundance of complexes **2** and **3** in their mixtures before separation by chromatography (checked by ^1H NMR) seems to depend on the nature of the phosphido ligand substituents. In the case of phenyl groups, the dibridged complex **3a** is formed in higher yield than the compound with two methyl groups (**3b**). In the case of the diphenylphosphido ligand an "exo" type structure (Chart 1, structure b) seems likely to be adopted. This exo type has been observed in some diphenylphosphido-bridged bimetallics derived from bent metallocenes.^{7,18} On the other hand, the "endo" type structures may be observed with the smaller methyl substituents (Chart 1, structure a). Two recent structure determinations confirm this endo substituent conformation: $\text{Cp}_2\text{Nb}(\text{CO})(\mu\text{-PMe}_2)\text{W}(\text{CO})_4(\text{PMe}_2\text{Ph})$ ¹⁵ and $\text{Cp}_2\text{Ta}(\text{CO})(\mu\text{-PMe}_2\text{S})\text{W}(\text{CO})_5$.¹⁹

Chart 1



The metallic center M of the $\text{M}(\text{CO})_n$ fragment lies in a favorable position for the formation of a second bridge in exo structure b, but the lateral position of this center in endo structure a renders the $\text{M}-\text{CO}(\text{Nb})$ interaction more difficult.

The complexes **2** and **3** are easily separated by chromatography, and **2** in THF solution converts rapidly to **3** upon irradiation. All these compounds have been characterized by ^1H and ^{31}P NMR and IR spectroscopy (Table 3).

The X-ray structure of $\text{Cp}_2\text{Nb}(\mu\text{-PPh}_2)(\mu\text{-CO})\text{Fe}(\text{CO})_3$ (**3a**) is the first to be carried out on a dibridged $\mu\text{-PPh}_2$ and $\mu\text{-CO}$ binuclear Nb-Fe complex derived from bent niobocenes.

Spectroscopic Studies. As expected, lower fields for ^{31}P resonances are recorded in the presence of phenyl groups (complexes a) than with methyl groups (complexes b). Lower fields are observed for monobridged complexes **2** than for their respective parent niobophosphines **1**. Upfield resonances in **2** are consistent with a large Nb-P-Fe angle,¹ indicative of a phosphido bridge across a nonbonded pair of metal atoms. It has been suggested that ^{31}P resonances of PR_2 ligands bridging a metal-metal bonding system appear downfield (+300 to +50 ppm), whereas upfield resonances (+50 to -300 ppm) are observed for compounds without a metal-metal bond.^{20,21} The ^{31}P resonances in our dibridged complexes **3** (225 ppm for **3a** and 190 ppm for **3b**) are shifted downfield by some 200 ppm with respect to the monobridged compounds **2**. The values of ^{31}P chemical shifts for complexes **3** argue strongly for the presence of a Nb-Fe bond.

An inspection of IR data in Table 3 gives some indications about the electronic structure of complexes **2** and **3**. They exhibit the typical patterns of $\text{M}(\text{CO})_4$ and $\text{M}(\text{CO})_3$ fragments. The $\nu(\text{CO})$ band (Nb-CO) of parent complexes **1a** and **1b** is affected little by complexation of the $\text{Fe}(\text{CO})_4$ fragment in **2a,b** but is dramatically shifted to lower frequencies in **3a,b**. This band, recorded for dibridged complexes **3** at 1751 cm^{-1} (**3a**) and 1738 cm^{-1} (**3b**), agrees with the presence of a semibridging or normal bridging carbonyl group. In all cases, the π coordination of the CO ligand (from a filled π orbital) to the second metal ($\pi(\text{CO}) \rightarrow \text{Fe}$) can be ruled out because the corresponding $\nu(\text{CO})$ vibration should be observed near 1550 cm^{-1} .²² The $\nu(\text{CO})$ frequencies of the $\text{Fe}(\text{CO})_4$ fragment (complexes **2**) exhibit a red shift ($\Delta\nu = 30\text{ cm}^{-1}$) with respect to those observed in the

(19) Challet, S.; Kubicki, M. M.; Leblanc, J. C.; Moïse, C.; Nuber, B. *J. Organomet. Chem.*, in press.

(20) Carty, A. J. *Adv. Chem. Ser.* **1982**, No. 196, 163.

(21) (a) Petersen, J. L.; Stewart, R. P., Jr. *Inorg. Chem.* **1980**, *19*, 186. (b) Carty, A. J.; MacLaughlin, S. A.; Taylor, N. J. *J. Organomet. Chem.* **1981**, *204*, C27. (c) Garrou, P. E. *Chem. Rev.* **1981**, *81*, 229.

(22) Pasyanskii, A. A.; Skripkin, Yu. V.; Eremenko, I. L.; Kalinrikov, V. T.; Aleksandrov, G. G.; Andrianov, V. G.; Struchkov, Yu. T. *J. Organomet. Chem.* **1979**, *165*, 49.

(14) Hoffmann, R. *J. Chem. Phys.* **1963**, *39*, 1397.

(15) Oudet, P.; Kubicki, M. M.; Moïse, C. *Acta. Crystallogr., Sect. C*, in press.

(16) Oudet, P.; Kubicki, M. M.; Perrey, D.; Moïse, C. To be submitted for publication in *Inorg. Chim. Acta*.

(17) Mealli, C.; Proserpio, D. M. *J. Chem. Educ.* **1990**, *67*, 399.

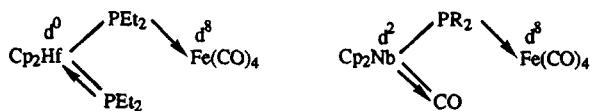
(18) Bonnet, G.; Kubicki, M. M.; Lavastre, O.; Leblanc, J. C.; Moïse, C. *Acta Crystallogr., Suppl.* **1990**, *A46*, C227.

Table 3. ^1H and ^{31}P NMR and IR ($\nu(\text{CO})$) Data for 1–4

complex	^1H (ppm, CD_3COCD_3)		^{31}P (ppm, CD_3COCD_3)	IR (cm^{-1} , THF)
	Cp	Ph or Me		
1a	5.08 (d), $J_{\text{HP}} = 1.5$ Hz	6.9–7.4 (m)	–2.9 (br)	1919 vs ^a
1b	5.03 (d), $J_{\text{HP}} = 1.5$ Hz	1.05 (d), $J_{\text{HP}} = 5.0$ Hz	–68.0 (br)	1910 vs ^a
2a	5.32 (d), $J_{\text{HP}} = 2.0$ Hz	7.1–8.2 (m)	35.4 (br)	2023 w, 1944 s, 1918 s, ^a 1901 s
2b	5.47 (d), $J_{\text{HP}} = 2.2$ Hz	1.72 (d), $J_{\text{HP}} = 7.0$ Hz	–21.3 (br)	2020 w, 1943 s, 1929 s, ^a 1901 s
3a	4.99 (d), $J_{\text{HP}} = 2.0$ Hz	7.4–8.2 (m)	225.5 (br)	1976 s, 1917 m, 1898 s, 1751 m ^a
3b	5.15 (d), $J_{\text{HP}} = 2.0$ Hz	2.10 (d), $J_{\text{HP}} = 8.5$ Hz	189.7 (br)	1969 s, 1924 m, 1897 s, 1738 m ^a
4a	5.29 (d), $J_{\text{HP}} = 1.5$ Hz	1.76 (d), $J_{\text{HP}} = 9.0$ Hz; 7.1–8.0 (m)	55.0 (br); 61.6 (d), $J_{\text{PP}} = 17$ Hz	1949 s, 1935 s, ^a 1860 s, 1843 s
4b	5.41 (d), $J_{\text{HP}} = 2.0$ Hz	1.70 (d), $J_{\text{HP}} = 6.5$ Hz; 1.75 (d), $J_{\text{HP}} = 9.0$ Hz; 7.3–7.9 (m)	–12.0 (br); 57.4 (d), $J_{\text{PP}} = 15$ Hz	1933 s, 1921 s, ^a 1851 s, 1844 s

^a $\nu(\text{CO})$ of Nb–CO.

Chart 2



mononuclear $\text{LFe}(\text{CO})_4$ compounds²³ (e.g. for $\text{L} = \text{PPh}_3$, $\nu(\text{CO})$ 2050, 1977, 1945 cm^{-1}). This means that metallophosphines 1 are electron rich and that a significant electron density is transferred from the $\text{Cp}_2\text{Nb}(\text{CO})$ fragment to the $\text{Fe}(\text{CO})_4$ one. Similar observations have been made for IR frequency shifts between the molybdenocene diphenylphosphine $\text{Cp}_2\text{Mo}(\text{H})\text{PPh}_2$ and the corresponding monobridged complexes $\text{Cp}_2\text{Mo}(\text{H})(\mu\text{-PPh}_2)\text{M}(\text{CO})_5$ ($\text{M} = \text{Cr}, \text{Mo}, \text{W}$).⁹ It is noteworthy that $\nu(\text{CO})$ frequencies observed in complexes 2 (Table 3) are essentially the same as those reported for the d^0 – d^8 complex $\text{Cp}_2\text{Hf}(\text{PEt}_2)(\mu\text{-PEt}_2)\text{Fe}(\text{CO})_4$ (2023, 1942, 1912, 1900 cm^{-1}).⁵ The possible bonding in Hf/Fe and in Nb/Fe complexes is presented in Chart 2.

In both cases the frontier orbital a_1 of the Cp_2M fragment (C_{2v} symmetry)²⁴ is populated. In the d^0 Hf complex the population of this orbital is assured by the electron lone pair of the PEt_2 ligand, while in the d^2 Nb compound the electron density is delocalized into the antibonding orbital of CO. Thus, it is possible that the electronic behaviors of $\text{Cp}_2\text{Hf}(\text{PEt}_2)$ and $\text{Cp}_2\text{Nb}(\text{CO})$ fragments are similar.

It has been observed that the $\nu(\text{CO})$ bands in *cis*- $\text{L}_2\text{-Fe}(\text{CO})_3$ compounds are recorded at lower frequencies ($\text{L}_2 = \text{dppp}$, $\nu(\text{CO})$ 1986, 1914, 1884 cm^{-1})²⁵ than for the monosubstituted tetracarbonyl complex $\text{LFe}(\text{CO})_4$. For our compounds 3 (*cis*- $\text{L}_2\text{Fe}(\text{CO})_3$ type) there are three possible ways for electron transfer from the metallophosphine: PR_2 and CO bridges and direct metal–metal interaction. Thus, the $\nu(\text{CO})$ vibrations in our dibridged derivatives $\text{Cp}_2\text{Nb}(\mu\text{-PPh}_2)(\mu\text{-CO})\text{Fe}(\text{CO})_3$ (3) would be expected to appear at lower frequencies than in $\text{L}_2\text{Fe}(\text{CO})_3$ and to be close to 1956–1884 cm^{-1} . However, the corresponding bands are observed at energies higher than the expected ones (Table 3). This indicates that some electronic density is transferred by the $\text{Fe}(\text{CO})_3$ unit to the metallocene fragment in 3. The results of EHMO calculations carried out on the $\text{Fe}(\text{CO})_n$ ($n = 3, 4$) fragments agree with IR data. The net negative charge retained on the $\text{Fe}(\text{CO})_n$ moiety is

higher in the case of tetracarbonyl (–0.651) than in that of tricarbonyl (–0.519).

The electron density retained on cyclopentadienyl rings of bent Cp_2M (M, d^2) fragments may be estimated with caution from the values of the corresponding ^1H NMR chemical shifts.²⁶ Data from Table 3 indicate that the density decreases in the order $3a > 1a > 2a$ (for diphenylphosphides) and $1b > 3b > 2b$ (for dimethylphosphides). In both series the lowest field resonances and consequently the lowest electron densities on Cp rings are observed for monobridged complexes 2. This is in rough agreement with EHMO calculations, which show that the net positive charges on Cp rings increase in the order $3 > 1 > 2$ (0.830, 0.915, and 0.928, respectively). The high-field ^1H resonances observed for complexes 3 confirm the transfer of electron density from the $\text{Fe}(\text{CO})_3$ unit to the Cp_2Nb one. The only way for such an electronic transfer to occur is by the π^* orbital of the carbonyl bridging ligand. It is worth noting that in the series of complexes derived from molybdenocene hydride “ Cp_2MoH ”, i.e. $\text{Cp}_2\text{Mo}(\text{H})\text{PPh}_2$ (**Mo1**), $\text{Cp}_2\text{Mo}(\text{H})(\mu\text{-PPh}_2)\text{M}'(\text{CO})_5$ (**Mo2**; $\text{M}' = \text{Cr}, \text{Mo}, \text{W}$), and $\text{Cp}_2\text{Mo}(\mu\text{-PPh}_2)(\mu\text{-H})\text{M}'(\text{CO})_4$ (**Mo3**), the order of decreasing electron density on Cp_2Mo fragment is **Mo1** > **Mo2** > **Mo3**.⁹ The different behavior of molybdenocene and niobocene derivatives is certainly due to the presence of the bridging carbonyl ligand in niobium complexes instead of the hydride in those of molybdenum. When terminal, this carbonyl ligand is involved in strong Nb to CO π back-bonding. The interaction of the HOMO frontier orbital of the Cp_2M fragment with the in-plane $\pi^*(\text{CO})$ symmetry-adapted MO is responsible for the high stability of the Nb–CO bond. This terminal carbonyl ligand can behave as a buffer, controlling the electronic properties of the $\text{Cp}_2\text{Nb}(\text{CO})$ fragment in different compounds. In our complexes 3, it may be easily expected that this in-plane $\pi^*(\text{CO})$ MO will efficiently control the fluctuation of electron density between metallic fragments. The lack of such a π^* system in molybdenum hydride complexes explains the downfield shifts of $^1\text{H}(\text{Cp})$ resonances in $\mu\text{-PPh}_2$ $\mu\text{-H}$ **Mo3** in contrast to our $\mu\text{-PR}_2$, $\mu\text{-CO}$ complexes 3.

The above interpretation of spectroscopic data may be supported by the shape of the second occupied molecular orbital (SOMO) shown in Figure 1b.

The in-plane π^* orbital of CO is clearly involved in the favorable overlaps with both metallic centers. The $12a_1$ (C_s point group) LUMO of the $\text{Fe}(\text{CO})_3$ fragment is mainly built of the d_{z^2} and d_{yz} atomic orbitals. In more

(23) (a) Darensbourg, D. J.; Nelson, H. H.; Hyde, C. L. *Inorg. Chem.* **1974**, *9*, 2135. (b) Howell, J. A. S.; Palin, M. G.; McArdle, P.; Cunningham, D.; Goldschmidt, Z.; Gottlieb, H. E.; Hezroni-Langerman, D. *Inorg. Chem.* **1993**, *32*, 3493.

(24) Lauher, J. W.; Hoffmann, R. *J. Am. Chem. Soc.* **1976**, *98*, 1729.

(25) Langford, G. R.; Akhtar, M.; Ellis, P. D.; MacDiarmid, A. G.; Odom, J. D. *Inorg. Chem.* **1975**, *14*, 2937.

(26) Kubicki, M. M.; Kergoat, R.; Guerschais, J. E.; Bkouche-Waksman, I.; Bois, C.; L'Haridon, P. *J. Organomet. Chem.* **1981**, *219*, 329.

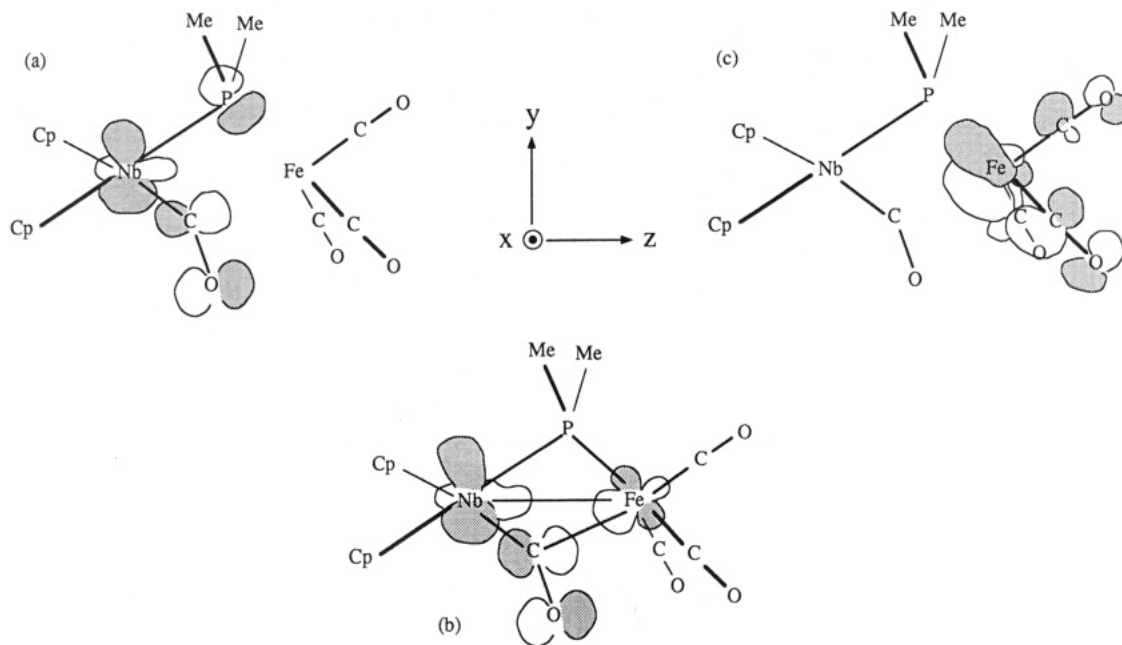


Figure 1. Formation of second occupied molecular orbital (SOMO, 35a') in **3b** (b) from the fragment molecular orbitals of $\text{Cp}_2\text{Nb}(\text{CO})\text{PMe}_2$ (HOMO, 24a') (a) and of $\text{Fe}(\text{CO})_3$ (LUMO, 12a') (c).

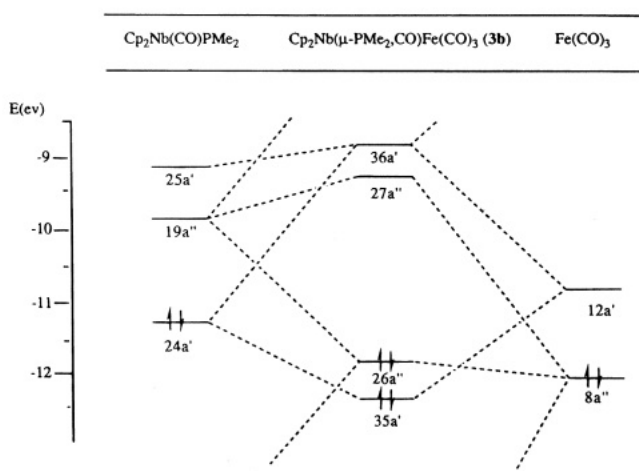


Figure 2. Correlation diagram of frontier orbitals for the formation of **3b** in C_s symmetry.

classical valence orbital description it may be assumed that the electron lone pair of the Nb^{III} atom localized in the $24a_1$ orbital interacts with the d_{z^2} AO of the iron atom. The resulting supplementary electron density on this atom can be further displaced into the d_{yz} AO, which interacts with a symmetry-adapted in-plane $\pi^*(\text{CO})$ orbital. The molecular orbital with bonding overlaps between Nb, $\mu\text{-CO}$, and Fe is formed. It is worth noting that the participation of the phosphido ligand (present in the HOMO of $\text{Cp}_2\text{Nb}(\text{CO})\text{PMe}_2$; Figure 1a) as well as of carbonyl ligands (present in the LUMO of $\text{Fe}(\text{CO})_3$; Figure 1c) no longer exists in the SOMO of **3b**. This is probably due to the favorable overlap between the niobium and iron centers. A correlation diagram for **3b** restricted to the frontier molecular orbitals is presented in Figure 2.

Figure 2 shows a stabilization of the HOMO in the $\text{Cp}_2\text{Nb}(\text{CO})\text{PMe}_2$ fragment by complexation to $\text{Fe}(\text{CO})_3$ and a slight destabilization of the HOMO of this last fragment, which becomes the HOMO of dinuclear molecule **3b**.

X-ray Structure of $\text{Cp}_2\text{Nb}(\mu\text{-CO})(\mu\text{-PPh}_2)\text{Fe}(\text{CO})_3$ (3a**).** The molecular structure of **3a** is shown in Figure 3. Selected bond distances and angles are set out in Table 4.

The Nb and Fe atoms are bridged by one PPh_2 ligand and one CO ligand. The Nb center shows the usual distorted-tetrahedral geometry characteristic of bent metallocenes, whereas the coordination geometry about Fe appears as distorted trigonal bipyramidal. The structure contains a planar $\text{Nb}(\mu\text{-C1O1})(\mu\text{-P})\text{Fe}$ arrangement (Figure 3b).

According to structural studies concerning a bridging CO ligand carried out by Cotton²⁷ and more recently by Crabtree,²⁸ the C1O1 group may be considered as a bent semibringing carbonyl, in agreement with theoretical studies of the nature of the carbonyl ligand in bimetallic systems.²⁹ Such a description of the bonding model is supported by the values of Nb—C1—O1 (141.53(9)°) and Fe—Nb—C1 (45.25(6)°) angles and Nb—C1 (2.174(10) Å) and Fe—C1 (2.053(10) Å) distances. When the difference in covalent radii of Nb and Fe is taken into account (1.66³⁰ and 1.34 Å,³¹ respectively), the C1O1 ligand is more strongly bonded to the niobium than to the iron. The Nb—P—Fe angle (75.42(1)°) in **3a** is close to the values of M—P—M angles found in dibridged complexes with a metal—metal bond: 75.03(3)° in $\text{W}_2(\text{CO})_8(\mu\text{-PPh}_2)_2$ ³² and 72.0° in $\text{Fe}_2(\text{CO})_6(\mu\text{-PPh}_2)_2$.³³ This last observation and the distance between Nb and Fe (Nb—Fe = 2.884(2) Å) in **3a** argue for the presence of the expected metal—metal bond.

The Nb—C1 distance of 2.174(10) Å in **3a** is longer

(27) Cotton, F. A. *Prog. Inorg. Chem.* **1976**, 21.

(28) Lavin, M.; Crabtree, R. H. *Inorg. Chem.* **1986**, 25, 805.

(29) Bénard, M.; Dedieu, A.; Nakamura, S. *Nouv. J. Chim.* **1984**, 3, 149.

(30) Andrianov, V. G.; Biryukov, B. P.; Struchkov, Y. T. *Zh. Strukt. Khim.* **1969**, 10, 1129.

(31) Churchill, M. R. *Perspect. Struct. Chem.* **1971**, 3, 91.

(32) Shyu, S. G.; Calligaris, M.; Nardin, G.; Wojcicki, A. *J. Am. Chem. Soc.* **1987**, 109, 3617.

(33) Ginsburg, R. E.; Rothrock, R. K.; Finke, R. G.; Collman, J. P.; Dahl, L. F. *J. Am. Chem. Soc.* **1979**, 101, 6550.

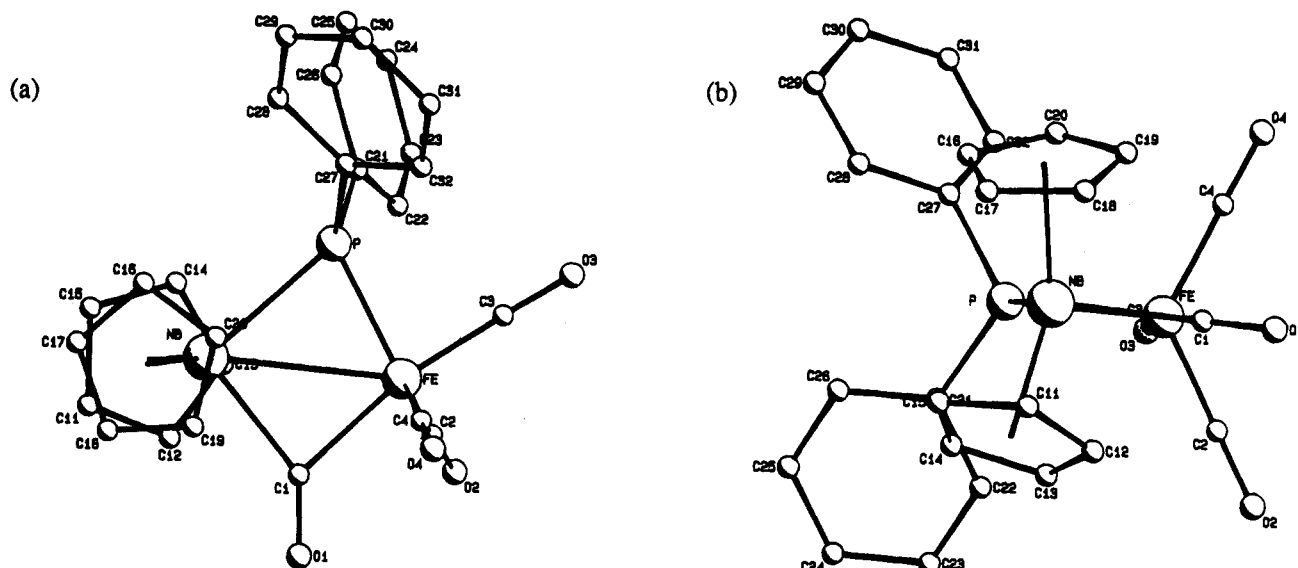


Figure 3. Molecular structure of $\text{Cp}_2\text{Nb}(\mu\text{-PPH}_2)(\mu\text{-CO})\text{Fe}(\text{CO})_3$ (**3a**): (a) projection on NbPFc1 showing the staggered conformation of Cp rings; (b) projection showing a planar arrangement of the NbPFc(C1O1) central unit.

Table 4. Selected Interatomic Distances (Å) and Bond Angles (deg) for $\text{Cp}_2\text{Nb}(\mu\text{-PPH}_2)(\mu\text{-CO})\text{Fe}(\text{CO})_3$ (**3a**)^a

Fe—Nb	2.884(2)	Fe—C3	1.729(12)
Fe—P	2.208(2)	Fe—C4	1.758(10)
Fe—C1	2.053(10)	Nb—C1	2.174(10)
Fe—C2	1.741(12)	Nb—P	2.492(10)
Nb—CP1	2.075	Nb—CP2	2.084
Nb—P—Fe	75.42(1)	C2—Fe—C3	89.27(5)
P—Fe—C1	105.52(3)	C2—Fe—C4	125.81(5)
P—Fe—C2	121.01(3)	C3—Fe—C4	95.69(5)
P—Fe—C3	85.13(4)	P—Nb—C1	93.06(3)
P—Fe—C4	113.18(4)	Nb—C1—O1	141.53(9)
CP1—Nb—CP2	132.2	Fe—Nb—P	47.81(6)
Fe—C1—O1	132.49(9)		

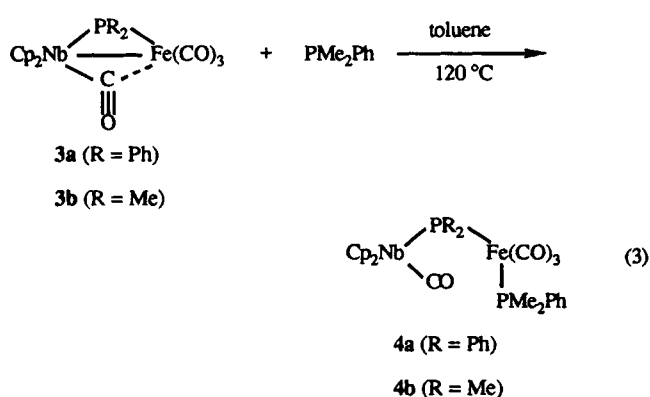
^a CP1 and CP2 represent the gravity centers of C11—C15 and C16—C20 cyclopentadienyl rings.

than the corresponding Nb—CO(terminal) bond lengths observed in the niobophosphine $\text{Cp}_2\text{Nb}(\text{CO})\text{P}^i\text{PrPh}$ (2.034(9) Å)¹¹ and in $\text{Cp}_2\text{Nb}(\text{CO})(\mu\text{-PMe}_2\text{W}(\text{CO})_4(\text{PMe}_2\text{Ph}))$ (2.055(18) Å).¹⁵ Strong π back-bonding (Nb^{III} electron lone pair to π antibonding in-plane CO orbital) is present in these last two complexes. The long Nb—C(CO) bond indicates clearly an expected modification of the nature of Nb—CO bonding in dibridged $\mu\text{-PR}_2$, $\mu\text{-CO}$ complexes.

Reactivity of Complexes 3 with CO and PMe_2Ph . After bubbling CO through a solution of **3** in refluxing toluene, we did not recover the expected phosphido-monobridged complexes **2**. The reaction was monitored by IR, and no change was observed after 3 h: the characteristic semibridging carbonyl bands (1751 cm^{-1} (**3a**) and 1738 cm^{-1} (**3b**)) were still present. However, a good donor ligand, such as PMe_2Ph , under the same conditions displaces the metal—metal bond, leading to the new monobridged compounds **4** in medium yields (eq 3).

¹H and ³¹P NMR and IR data for complexes **4** are in Table 3.

Bonding of the PMe_2Ph ligand to Fe rather than Nb is indicated by the absence of a doublet of doublets or a triplet for the ¹H resonances of cyclopentadienyl ligands in complexes **4**: the signal is a doublet ($J_{\text{PH}} = 1.5$ Hz (**4a**) and 2 Hz (**4b**)). ¹H resonances of cyclopentadienyl



protons in **4** (5.32–5.47 ppm) are similar to those found for complexes **2** (5.29–5.41 ppm), indicating a similar electronic density retained on the Cp₂ unit. This is confirmed by EHMO calculations on the model of complexes **4**, which show that the net charge retained on the Cp₂ fragment is equal to +0.922: it is only 0.006 lower than the charge calculated for the complexes **2** (+0.928).

Complexes **4** show four $\nu(\text{CO})$ stretching vibrations (one due to the CO bonded to Nb), indicating a cis position of the two phosphorus atoms in the coordination geometry of Fe. The values of their frequencies are shifted by some 50 cm^{-1} (red shift) with respect to those observed in the $\text{Fe}(\text{CO})_3(\text{dppp})$ complex.²⁵ This confirms our suggestions that metallophosphines **1** are electron rich and behave as good electron donors and that the nucleophilicity of the phosphorus atom therein is enhanced.

³¹P NMR spectra now show two resonances: one broad signal (61.6 ppm, **4a**; -12 ppm, **4b**) due to the phosphido bridge (interaction with the quadrupolar ($I = 9/2$) ⁹³Nb nucleus) and one doublet (55 ppm, ²J_{PP} = 17 Hz, **4a**; 57.3 ppm, ²J_{PP} = 15 Hz, **4b**) due to the coordinated PMe_2Ph ligand. The same range of coupling constants is observed in other *cis*-P₂Fe(CO)₃ systems.^{34,35} The upfield ³¹P resonance of the broad signal

(34) Yu, Y. F.; Galluci, J.; Wojcicki, A. *J. Am. Chem. Soc.* **1983**, *105*, 4826.

(+61.6 ppm, **4a**; -12 ppm, **4b**) with respect to that recorded for complexes **3** is consistent with the cleavage of the Nb-Fe bond.

Conclusion

As expected, the terminal phosphido derivatives of bis(cyclopentadienyl)niobium $\text{Cp}_2\text{Nb}(\text{CO})\text{PR}_2$ (R = Ph, Me) easily bind the metal carbonyl fragment $\text{Fe}(\text{CO})_4$ (from $\text{Fe}_2(\text{CO})_9$) to form new heterobimetallic complexes with or without a metal-metal bond. The spectroscopic and X-ray structural results both suggest that the dibridged $\mu\text{-PR}_2$ and $\mu\text{-CO}$ complexes contain bonded $18e^- \text{Nb}^{\text{III}}$ and $18e^- \text{Fe}^0$ centers. One of the consequences of the semibridging nature of the carbonyl ligand is that the excess electronic density retained on

$\text{Fe}(\text{CO})_3$ in complexes **3** can be easily transferred to the Cp_2Nb unit. This effect cannot operate in the case of equivalent molybdenum compounds with a hydrido bridge. The results obtained by $^1\text{H}(\text{Cp}_2)$, IR, and EHMO methods are in good agreement. Preliminary reactivity studies of dibridged complexes with a metal-metal bond $\text{Cp}_2\text{Nb}(\mu\text{-PR}_2)(\mu\text{-CO})\text{Fe}(\text{CO})_3$ (R = Ph, Me) carried out with CO and PMe_2Ph show that the metal-metal bond is a rather strong one.

Acknowledgment. We thank Miss Christine Martin for EHMO calculations.

Supplementary Material Available: Tables of anisotropic thermal parameters, hydrogen atom coordinates, all bond distances and angles, and least-squares planes (5 pages). Ordering information is given on any current masthead page.

OM940210I

(35) Nixon, J. F.; Pidcock, A. *Annual Review of NMR Spectroscopy*; Academic Press: London, 1969; Vol. 2, p 346, and references therein.